Dynamics of a bouncing ball in human performance

Dagmar Sternad
Department of Kinesiology, 266 Recreation Building, Pennsylvania State University, University Park, Pennsylvania 16802

Marcos Duarte
Universidade de São Paulo, Avenida Mello Moraes 65, 05508-900 São Paulo, Brazil

Hiromu Katsumata
Department of Kinesiology, Pennsylvania State University, University Park, Pennsylvania 16802

Stefan Schaal
Department of Computer Science, University of Southern California, Los Angeles, California 90089-2520
(Received 28 June 2000; published 19 December 2000)

On the basis of a modified bouncing-ball model, we investigated whether human movements utilize principles of dynamic stability in their performance of a similar movement task. Stability analyses of the model provided predictions about conditions indicative of a dynamically stable period-one regime. In a series of experiments, human subjects bounced a ball rhythmically on a racket and displayed these conditions supporting that they attuned to and exploited the dynamic stability properties of the task.

DOI: 10.1103/PhysRevE.63.011902 PACS number(s): 87.19.St, 05.45.Gg

I. INTRODUCTION

A ball bouncing on an oscillating table is a frequently studied model system to explore and demonstrate the properties of nonlinear dynamic systems, such as fixed points, periodic and strange attractors, and period-doubling bifurcations to chaos [1]. The model system has been applied to various problems in physical systems and in engineering, ranging from quantum physical problems such as the Fermi-Ulam model to transportation of granular solids on conveyor belts [2,3]. The major interest in the ball-bouncing system has been directed to the chaotic features of the model and their experimental replication [4]. Despite this diversity, only few studies have ventured to transfer these theoretical insights to more macroscopic applications such as the control of actuator movements of robots [5]. That ball bouncing is also a relevant formal model for understanding human movement control was demonstrated by Schaal, Sternad, and Atkeson [6]. The skill of bouncing a ball rhythmically on a planar surface like a racket is a perceptual-motor task that poses all the fundamental questions raised in the study of human movement coordination. To bounce or ''juggle'' a ball rhythmically in the air requires the fine control of the vertical movements of the racket in order to hit the ball with the appropriate velocity at the right place and the right time with respect to the ball's trajectory. The question in focus is whether rhythmic performance is guided by stability properties of the mechanics of the task. An important difference between analyzing human movement and physical experimental systems is that while the variables and parameters of physical experiments are under the experimenter's control, human subjects when bouncing a ball have to solve the problem by choosing a ''parametrization'' of their system in order to attain stability. Empirical data have to be evaluated with respect to the model's prediction to test whether the parameter selection process of humans is indeed sensitive to such attractive regimes as defined by the ball-bouncing map.

That human movements obey principles of dynamic stability was already demonstrated in the skill of juggling three and more balls with two hands [7]. In formal and empirical analyses it was shown that in rhythmic stable performance, specific component times of the hands' and balls' cycles showed properties of phase locking. In deliberately close correspondence to the physical model of one-dimensional (1D) ball bouncing, Schaal *et al.* [6] investigated the task of one-handed bouncing of a ball with a racket, postulating that humans attune to the attractive properties of period-one bouncing and exploit the dynamic stability of this task. This coordination strategy has the advantage that perturbations ''passively'' converge back to the stable attractor, which therefore obviates the need for active error corrections. This strategy stands in contrast to the approach of classical control theory in which a perturbation of the ball would be compensated for by an explicit change of the actuator trajectory. Although this conceptual framework still prevails in the attempts to understand human movement control, it has the disadvantage of demanding highly accurate sensing and precise control, two characteristics that are not typical for biological performance and that can be computationally rather demanding in complex movement systems. An alternative approach has arisen from the nonlinear dynamical system perspective, which assumes that humans utilize stability properties of the nonlinear dynamic system, rather than overrule them, and thereby find potentially more economical coordination.

In this paper, we briefly present the modeling approach as developed and modified for studying human ball bouncing. Following a previous study, which gave a first indication in a highly constrained experimental task that human subjects do indeed exploit dynamic stability properties of the vibratory ball-table system, we present four new experiments that demonstrate the robustness of these results. The first experi-

ment relaxed the experimental constraints of the task and reproduced all the findings supporting dynamic stability. In the second experiment, subjects juggled the ball freely in 3D. The third experiment examined whether during a learning process the critical variable indicating dynamic stability is optimized. A last experiment aimed to challenge the stability of performance by depriving subjects of different perceptual information. We showed that while dynamic stability remains a central criterion, additional stabilizing adjustments complement the strategy. Kinetic information about the impact appears to provide the most salient information to attune to dynamic stability.

II. THE MODEL

Bouncing a ball with a racket was modeled as a planar surface performing periodic vertical movements impacting a ball repeatedly, similar to the classical model of a vibratory table bouncing a particle [1]. A key difference, though, is that the racket's movement in our real experiments was not a single sinusoidal function and therefore the model allowed for any arbitrary periodic movements of the table expressed by a Fourier series. The often applied ''high bounce'' approximation, assuming invariant position at impact and symmetric parabolic flight trajectories of the ball due to negligible racket amplitude, is not suitable for the experimental movements as seen below. Therefore, the model's motion was expressed in terms of a two-dimensional state vector, i.e., racket position and velocity, rather than phase. To facilitate comparison of the model with actual data, the equations were not put into dimensionless form as in the classical dissipative standard map (known as the modified Fermi-Ulam problem [8] or Zaslavskj-Rachko mapping [9]).

Assumptions of the model are arbitrary periodic motion of the surface, ballistic flight of the ball, instantaneous impact modeled by a coefficient of restitution, and a mass of the racket that is considerably larger than the ball's such that the racket trajectory is not affected by the impact. In the Poincaré map $\Sigma=\{(x_B,\dot{x}_B,x_R,\dot{x}_R)\in R^4|x_B-x_R=0\}$, the equations of motion can be expressed in discrete notation in reference to the *nth* impact [6]:

$$x_{B,n+1}=x_{R,n+1} \quad \text{and} \quad x_{R,n+1}=x_{R,n+1}(t_n), \tag{1a}$$

$$\dot{x}_{B,n+1}=-\sqrt{[(1+\alpha)\dot{x}_{R,n}-\alpha\dot{x}_{B,n}]^2-2g(x_{R,n+1}-x_{R,n})}, \tag{1b}$$

$$0.5gt_n^2-[(1+\alpha)\dot{x}_{R,n}-\alpha\dot{x}_{B,n}]t_n+(x_{R,n+1}-x_{R,n})=0. \tag{1c}$$

t_n denotes the times at successive impacts; $x_{B,n}$, $x_{R,n}$, $\dot{x}_{B,n}$, $\dot{x}_{R,n}$ are the vertical positions and velocities of ball and racket at the nth impact; α is the coefficient of restitution; and g is the acceleration due to gravity. These equations are not solvable because the racket's position at impact $n+1$ is not known at time n. However, stability analyses can be applied to find criteria under which the system achieves stable solutions, where the period-one solution corresponds to the task in our experiments. Provided smooth Periodic

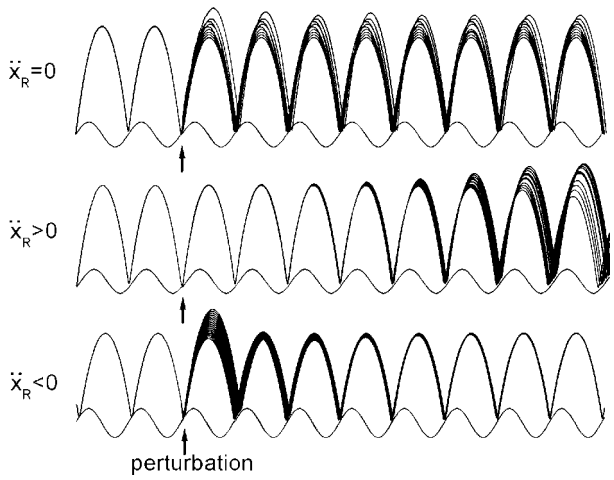

FIG. 1. Simulation of Eq. (1). The three runs demonstrate (a) the neutrally stable regime, $\ddot{x}_R=0$, where a perturbation remains unchanged; (b) the unstable regime, $\ddot{x}_R>0$, where perturbations amplify; and (c) the stable regime $\ddot{x}_R<0$, where perturbations converge back to the attractor.

Table motion and $\dot{x}_{R,n}$ exceeding a minimum value to compensate for the energy loss at impact, local linear stability analysis determined at least one asymptotically stable fixed point. The racket's acceleration at impact $\ddot{x}_{R,n}$ has to satisfy the nontrivial condition:

$$-2g\frac{1+\alpha^2}{(1+\alpha)^2}<\ddot{x}_{R,n}<0. \tag{2}$$

As g and α are constants, $\ddot{x}_{R,n}$ is the major variable that determines the stability of the solution. Additionally, a nonlocal Lyapunov stability analysis was performed on Eq. (1) linearized around equilibrium points in order to numerically determine the degree of stability for 20 values within this relatively large range given by Eq. (2) (for details, see the Appendix). As dynamical stability is closely related to variability, this numerically derived stability index serves as an inverse index for performance variability of the juggling trials.

Two major predictions were derived. (i) Dynamically stable performance is obtained if the mean racket acceleration at impact $\ddot{x}_R$ satisfies $\ddot{x}_R\in[-11.44\ \mathrm{ms}^{-2},-0\ \mathrm{ms}^{-2}]$. This range is determined for $\alpha=0.42$, which is the coefficient of restitution for the first experiment. Figure 1 illustrates the behavior using a simulation of Eq. (1). (a) If $\ddot{x}_R$ is zero, small initial differences or perturbations remain unchanged throughout the run and the system is neutrally stable. (b) If $\ddot{x}_R$ is positive, small initial differences or perturbations amplify and lead to loss of stability, if no corrective adjustments are made. (c) If $\ddot{x}_R$ is negative, small initial differences or perturbations diminish and converge towards an invariant dynamically stable performance. (ii) The degree of stability is a nonlinear function of $\ddot{x}_R$, with a region of relatively high stability in the approximate range $\ddot{x}_R\in$

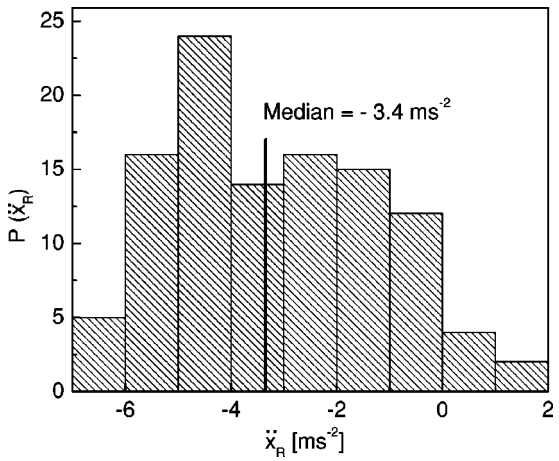

FIG. 2. Experiment 1: Histogram of racket accelerations at impact, $\ddot{x}_R$. Plotted are the trial mean values of all subjects.

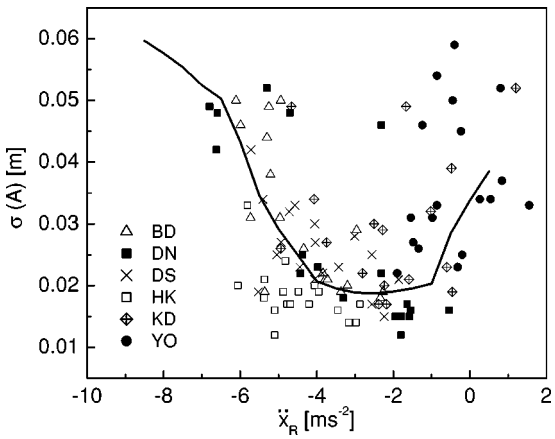

FIG. 3. Experiment 1: Standard deviations of ball amplitudes throughout a 30-sec-long trial, $\sigma(A)$, plotted against trial means of $\ddot{x}_R$. The different symbols represent different subjects. The solid line represents the predicted degree of stability as calculated by the Lyapunov analysis.

$[-6\ \mathrm{ms}^{-2}, -2\mathrm{ms}^{-2}]$. For the experiment, the inverse of this measure is used and equated with variability. Figure 3 includes the results of the Lyapunov analysis where the curved solid line represents the predicted shape for variability. Evidently, the range of dynamically stable values of $\ddot{x}_R$ and the region of optimal stability changes with α and g. Relevant for the reported experiments is that the range of stable values of $\ddot{x}_R$ decreases with higher α. The shape of the function approximately scales with the range.

Note that these predictions run counter to the hypothesis that human movements maximize efficiency. Under this hypothesis, the ball should be contacted at the moment of peak velocity, corresponding to $\ddot{x}_R = 0$, which would lead to the highest possible amplitude for a given racket trajectory. If, instead, the ball is impacted at the decelerating trajectory segment, peak velocity has to be higher in order to achieve the same ball amplitude. Hitting the ball in the decelerating phase of the racket trajectory is also an unusual solution from a control theoretic point of view. As reviewed in [6], robotic studies of ball bouncing never discovered the dynamically stable regime of the task, but rather selected marginally or even unstable regimes for ball bouncing, at the cost of having to include a complex feedback control strategy. Thus, negative acceleration at impact is a nontrivial prediction. If found in human performance, it most likely signifies that humans attune to the dynamic stability of the task rather than use an elaborate feedback control strategy.

In a previous study, Schaal *et al.* [6] provided first support for these predictions. The experiment was performed with a special apparatus where subjects were instructed to bounce a ball rhythmically with a steady ball amplitude by moving the handle of a 1-m-long lever arm with a racket attached at the other end. A pantograph linkage ensured that the racket's surface remained strictly horizontal. The ball was affixed to a 1-m-long boom to confine its trajectory to a (curvi)linear path. Hand and racket as well as ball trajectories were thereby strictly confined to the vertical dimension, in close correspondence to the model. Accelerations were obtained by numerical differentiation of the position signal. The results for six subjects verified that mean $\ddot{x}_R$ across the successive impacts of one trial was in the range that predicted optimal stability, with an overall mean of $-3.44\ \mathrm{ms}^{-2}$. The variability associated with subjects' $\ddot{x}_R$ values, operationalized as standard deviations of repeated impacts within one trial, followed the predictions of the Lyapunov analysis. As the task and the human movements were highly constrained, the question arises whether in less constrained settings these results will be upheld. This was the purpose of the first two experiments.

III. EXPERIMENT 1: UNCONSTRAINED ARM MOVEMENTS AND RACKET ORIENTATION

Six subjects were instructed to bounce a ball rhythmically with a hand-held racket in the air such that the ball amplitude was invariant over repeated impacts throughout the 30-sec-long trial, a pattern corresponding to a stable period-one solution. The ball was affixed to a 1.3-m-long boom to confine its trajectory to a (curvi)linear path. A potentiometer, attached to the axis of rotation, measured the angular displacement of the ball. The racket's acceleration was measured by an accelerometer attached to the racket's surface; its vertical displacement was measured by a thin string spring-rolled around a coil on the floor with an attached potentiometer. Note that although the movements of the subject's racket were unconstrained and the surface of the racket was no longer fixed to the horizontal orientation, it was sufficient to measure only the racket's vertical displacement and acceleration. Subjects performed six trials for each of three amplitudes (low, preferred, and high), which were within the linear range of the ball's trajectory. The conditions were performed in random order. The principal movement parameter was the racket's acceleration at ball impact. The mean $\ddot{x}_R$, calculated over the approximately 30 impacts during one trial, served as the empirical equivalent for the predicted acceleration. The degree of stability was captured by using the task criterion of invariant ball amplitude. The variability of the ball amplitude was operationalized in terms of standard deviations of the

ball amplitude across each trial, $\sigma(A)$.

Results. Figure 2 shows a histogram of the mean values of $\ddot{x}_R$ for all trials and all subjects. The distribution demonstrates that subjects predominantly preferred movement solutions with negative $\ddot{x}_R \in [-6\ \mathrm{ms}^{-2}, -2\ \mathrm{ms}^{-2}]$ with a median at $-3.40\ \mathrm{ms}^{-2}$. It is noteworthy that 6 of the 108 trials had positive $\ddot{x}_R$ showing that the choice of $\ddot{x}_R < 0$ is not trivial. Figure 3 shows the same trial means of $\ddot{x}_R$ plotted against $\sigma(A)$. The different symbols identify the six subjects who generally form clusters at selected subsets of values. Across subjects, the $\ddot{x}_R$ values covered a large portion of the range of predicted optimal stability. Interestingly, one subject (YO) tended to choose movement regimes at the boundary of stability. This subject had very little experience with racket sports, in comparison to the subject HK, who was an experienced tennis player. In order to understand the more scattered distribution of $\ddot{x}_R$ values in the remaining four subjects, we investigated the time course of the $\ddot{x}_R$ trial means across the sequence of 18 trials of each subject. Two subjects (KD and BD) showed a tendency to approach a preferred value towards the end of the experiment ($-2\ \mathrm{ms}^{-2}$ and $-5.5\ \mathrm{ms}^{-2}$, respectively). However, these results were not significant, probably because of the random sequence of amplitude conditions (see below).

Additionally, Fig. 3 shows that trial variability associated with the trial means and operationalized in $\sigma(A)$ showed a U-shaped dependency. This scatter clustered around the solid line, which represents the predictions of variability from the numerical Lyapunov analysis. Note, though, that while the values of $\sigma(A)$ are in units of m, the values of the nonlocal predictions are in arbitrary units and were scaled to the amplitude of the data. Although only a qualitative comparison, the close fit with the predicted U shape supported the predictions. The difference between YO and HK as well as between other subjects was also reflected in the variability (standard deviations) of impact period and racket amplitudes per trial. This confirms that the value of $\ddot{x}_R$ is a sensitive measure for stability of performance. Further support for the pivotal role of dynamic stability in the subjects' performance was provided by a comparative analysis of the six trials performed in one amplitude condition. For the six trials of each amplitude condition, the $\ddot{x}_R$ values, averaged across all six subjects, showed a significant decrease from more positive to more negative values. Thus, a short-term learning process across six trials demonstrated that subjects progressively attuned towards a performance variant which offered higher stability.

IV. EXPERIMENT 2: FREE BOUNCING IN 3D

In order to further pursue how robust these results are, a second experiment was run in which subjects performed ball bouncing freely in 3D. Using the same tennis racket with the attached accelerometer, the crucial modification was that the ball was no longer attached to the boom. The accelerometer attached to the racket had a long cable connecting it to the computer, so that the racket movements were not obstructed

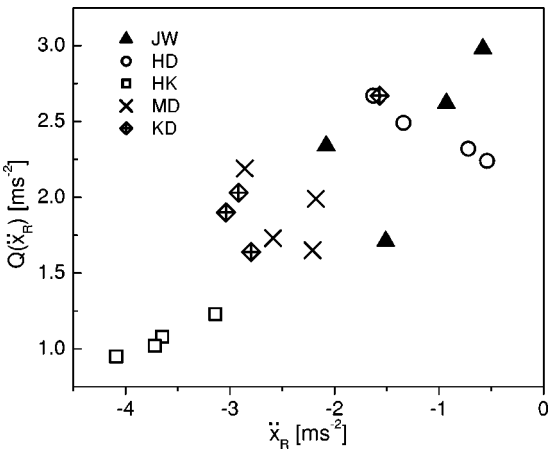

FIG. 4. Experiment 2: Quartile range of racket accelerations at impact throughout a 30-sec-long trial, $Q(\ddot{x}_R)$, plotted against trial medians of $\ddot{x}_R$ in the experiment where task restrictions were removed and bouncing was performed in 3D. The different symbols represent different subjects.

and were truly performed in 3D. A sponge ball of the size of a tennis ball was used with $\alpha = 0.52$. Subjects were asked to find their most comfortable ball amplitude and maintain it throughout the 30-sec-long trial. They were also instructed to stay as stationary as possible and not to do more than one step to reach the ball when it was displaced slightly.

Results. Participants performed trials with median $\ddot{x}_R$ values ranging between $-4.10\ \mathrm{ms}^{-2}$ and $-0.54\ \mathrm{ms}^{-2}$ [10]. As summarized in Fig. 4, different participants had trial means around different values that reflected different preferences, which repeated the picture obtained from experiment 1. This result confirmed that the model's predictions were again satisfied. What is noticeable, though, is that $\ddot{x}_R$ values were confined to a smaller range than previously. As can be computed from Eq. (2), the larger α, the shorter the range, or the smaller the ''well'' providing optimal stability. To test the predictions for variability associated with different $\ddot{x}_R$ values, the same qualitative picture as in experiment 1 emerged. As no position data of the ball and racket were collected, variability was quantified in terms of the quartile range of $\ddot{x}_R$. $Q(\ddot{x}_R)$ consistently decreased with increasingly negative $\ddot{x}_R$ values. Note again that individual subjects rank differently: Subject JW had no experience with racket sports, while HK was the same subject who had experience in tennis as well as in the special experimental task. This result further highlighted that acceleration values are modified through practice towards values closer to the predicted optimal range.

In sum, both experiments verified that the model of a bouncing ball provided a useful abstraction to gain some insight into the human perceptual-motor task of ''ball juggling.'' Further, criteria for dynamic stability derived from the nonlinear impact map can be generalized to a task which allows 3D motions of the effector. Human subjects appeared to exploit this stability in their control of rhythmic performance. Moreover, long-term experience and short-term practice revealed significant interindividual differences and changes across trials, respectively. Therefore, a third experi-

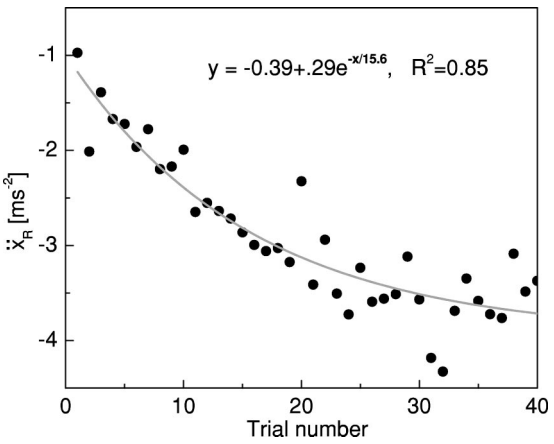

FIG. 5. Experiment 3: Racket accelerations at impact $\ddot{x}_R$ across a series of 40 30-sec-long trials. Each data point represents the average of six subjects' trial means. The solid line represents the exponential fit with the coefficients and R^2 listed at the bottom.

ment followed that directly tested whether impact acceleration changed across a series of trials. Based on previous results, it was hypothesized that subjects attune to dynamic stability across a short-term learning process.

V. EXPERIMENT 3: EFFECTS OF PRACTICE

Using the same experimental apparatus as in experiment 1, subjects were asked to perform a sequence of 40 trials of 30-sec duration each. They could select their preferred amplitude but were then asked to maintain this amplitude throughout all trials of the experiment. There were short rest periods between the individual trials. To avoid fatigue, the 40 trials were performed in two blocks; half of the trials were performed by the right and left hand, respectively. The order of blocks was counterbalanced across the six subjects.

Results. Figure 5 shows the average results of all six subjects across the 40 trials. There is a highly significant exponential decrease in the average $\ddot{x}_R$ towards more negative values of $\ddot{x}_R$. Importantly, the variability of $\ddot{x}_R$, operationalized in standard deviations, only slightly decreased with trial number. This again highlights the pivotal nature of the magnitude of $\ddot{x}_R$.

In a final step, we asked what kind of information subjects rely on in order to ''find'' this dynamically stable solution, or whether dynamic stability is compromised when the human actor is challenged by depriving perceptual information.

VI. EXPERIMENT 4: PERCEPTUAL MANIPULATIONS IN 1D BALL BOUNCING

Using the same apparatus as in Schaal *et al.* [6], three subjects were instructed to bounce a ball rhythmically with a steady ball amplitude. Three perceptual conditions were imposed: excluding visual information, no-VI (participants closed their eyes), excluding kinesthetic information about the impact no-KI, and a control condition with full perceptual information FI. To exclude kinesthetic information about the impact, a telerobotic device was attached to the ''juggling arm,'' which recorded its angular displacements, which then served as desired trajectories for a ''robot'' to move the actual racket. Thereby, subjects moved the handle observing the racket contacting the ball but without getting tactile information about the ball contact. All perceptual conditions were performed with three different ball amplitudes

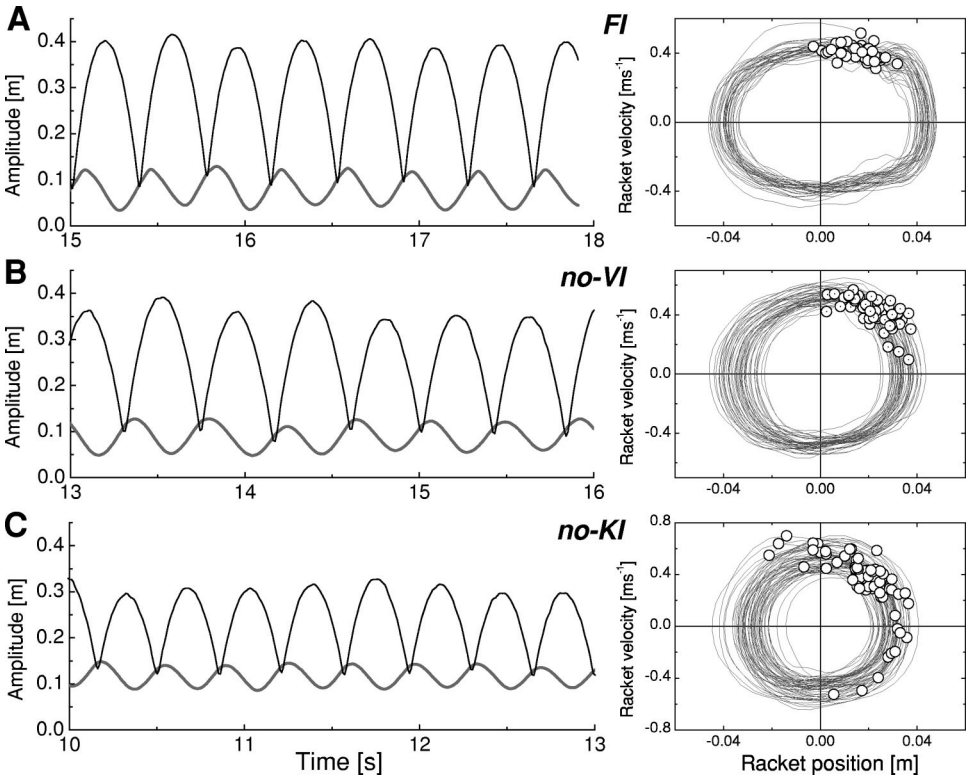

FIG. 6. Experiment 4: Three time series and their respective phase portraits of exemplary trials performed in the three perceptual conditions. The dots in the phase portraits denote the impacts.

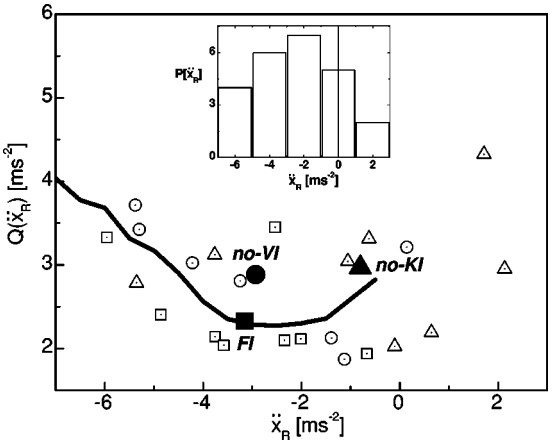

FIG. 7. Experiment 4: Quartile range, $Q(\ddot{x}_R)$, versus median values of $\ddot{x}_R$ obtained for each trial performed under three perceptual conditions of three subjects. The enlarged points represent the means across the three perceptual conditions within each subject. The solid line represents the predictions from the Lyapunov analysis.

for 30 s each, with two repetitions for each condition.

Results. Exemplary time series of ball and racket displacements and the corresponding phase portraits of the same trials are shown for the three different perceptual conditions in Fig. 6. The ball-racket impact positions clearly varied across the trial and demonstrated that the often applied modeling assumption about symmetric parabolic ball trajectories was not appropriate here. Also, the racket's displacement profile was not exactly sinusoidal. The dots in the phase portraits visualize the impacts within one trial showing predominantly negative values for $\ddot{x}_R$ in the predicted range: $\ddot{x}_R \in [-6\ \mathrm{ms}^{-2}, -2\ \mathrm{ms}^{-2}]$. The FI condition [Fig. 6(a)], where no perceptual restrictions were imposed, showed a tight cluster of $\ddot{x}_R$ around a median $\ddot{x}_R = -4.16\ \mathrm{ms}^{-2}$ and signified a dynamically stable solution, again replicating previous results [6]. The no-VI condition [Fig. 6(b)] was characterized by median $\ddot{x}_R$ values around $-4.43\ \mathrm{ms}^{-2}$, but this predominantly stable solution was generally less consistent. Note, that it was only for the very short moment of contact that kinetic information about the impact was available. In contrast, when continuous kinematic information about the ball's trajectory throughout the entire cycle was available, but no kinetic information in no-KI [Fig. 6(c)], $\ddot{x}_R$ values frequently scattered into the positive range (median $\ddot{x}_R = -0.31\ \mathrm{ms}^{-2}$).

Quantitative comparison of three perceptual conditions for all trials and subjects revealed significant differences in the median $\ddot{x}_R$ values and their variability. Median and quartile range of $\ddot{x}_R$, calculated per trial, served as empirical estimates to test the model's predictions statistically. Figure 7 shows all individual trial medians as well as the averages for the three individual subjects in the three perceptual conditions. The solid line represents predictions from the Lyapunov analysis. The inserted figure shows the histogram of the trial medians of $\ddot{x}_R$ with its respective median at $-2\ \mathrm{ms}^{-2}$. All subjects showed the same relational pattern of the median and quartile ranges of $\ddot{x}_R$. The differences in the median and quartile ranges of $\ddot{x}_R$ between the three subjects reflected their respective experience with racket sports. Yet, common to all three subjects was the fact that the medians of $\ddot{x}_R$ were different for the three conditions in the order: FI $<$no-VI$<$no-KI. When only visual information was accessible (no-KI), many trials were performed with $\ddot{x}_R > 0$, signifying dynamically unstable solutions. This result indicated that kinetic information about the impact was more necessary than visual information, although the latter gave information about the continuous kinematic trajectory of the ball. Yet, despite being close to an unstable regime, the variability in no-KI still remained low and therefore suggested that subjects employed a different strategy, probably aided by visual information, that corrected potential errors resulting from perturbations. $Q(\ddot{x}_R)$ was lowest in FI, but not statistically different for no-VI and no-KI. The difference in $Q(\ddot{x}_R)$ between FI and no-VI or the comparable results in $Q(\ddot{x}_R)$ in no-VI and no-KI cannot be explained by the model. This result points to the fact that in FI, additional visually guided adjustments must be made to reduce the variability.

In conclusion, a modified impact map for the ball-bouncing system was used to extract predictions to test whether humans, when performing a similar task, attune to dynamically stable regimes. Results confirmed these hypotheses not only for highly constrained but also for unconstrained movements. When subjects are deprived of either kinetic or kinematic information, kinetic information is shown to provide the major source of information for parametrizing the movement system to this stable regime. When kinematic information was the principal source, subjects tended to fall back on other, probably anticipatory and corrective, control strategies.

ACKNOWLEDGMENTS

This work was made possible by the National Science Foundation (D.S.). Marcos Duarte is grateful to the Fundação de Amparo à Pesquisa do Estado de São Paulo–FAPESP/Brazil.

APPENDIX

Local linear stability

Local linear stability analysis gives a first assessment of the stability properties of the fixed points determined for the model system (Eq. 1). Linearizing about an equilibrium point results in a matrix equation for the ball:

$$\mathbf{x}_{B,n+1} = \mathbf{A}\mathbf{x}_{B,n.} \tag{A1}$$

The characteristic 2×2 matrix $\mathbf{A}$ has two eigenvalues λ_1, λ_2. The condition for stable equilibrium points in discrete systems is that the absolute value of both eigenvalues must lie in the interval $[0,1]$. It therefore suffices to test the

larger absolute eigenvalue, $|\lambda_{max}|$, for this condition and distinguish amongst the following three cases within the range of $\ddot{x}_{R,n}$:

$$0>\ddot{x}_{R,n}\geqslant -g\frac{(1-\alpha)^2}{(1+\alpha)^2}: \quad 1>|\lambda_{max}|\geqslant\alpha, \tag{A2a}$$

$$-g\frac{(1-\alpha)^2}{(1+\alpha)^2}>\ddot{x}_{R,n}>-g: \quad |\lambda_1=\lambda_2=\lambda_3|=\alpha, \tag{A2b}$$

$$-g\geqslant\ddot{x}_{R,n}>-2g\frac{1+\alpha^2}{(1+\alpha)^2}: \quad 1>|\lambda_{max}|\geqslant\alpha. \tag{A2c}$$

The equations show that local stability only depends on the racket's acceleration at impact, $\ddot{x}_{R,n}$, the coefficient of restitution, α, and the gravity acceleration g. While α and g are constant for a given experiment and not under the control of an effector system, $\ddot{x}_{R,n}$ will serve as the main variable for the assessment of different bouncing solutions in the experiment. For the analytical evaluation of local stability, the range of $\ddot{x}_{R,n}$, where $|\lambda_{max}|$ is at a minimum, is of primary importance. For given values of α, the range is defined. For instance, for $\alpha=0.42$, the range is $[-11.44\ \mathrm{ms}^{-2},0\ \mathrm{ms}^{-2}]$. However, this range is rather large and local stability analysis does not differentiate between conditions. Hence, a nonlocal stability analysis is required to further classify these locally stable solutions. A prerequisite for this analysis is that different solutions can be compared, i.e., normalized, such that quantitative comparisons are possible. Mathematically, this question is addressed by topological orbital equivalence (TOE), which tests whether one dynamical system can be continuously transformed into another one.

Topological orbital equivalence

A formal way of establishing TOE is to find an orientation-preserving homeomorphism between two dynamical systems [11,12]. The following scaling relation h:

$$h:=\begin{cases}\dot{x}'_{B,n}=c\dot{x}_{B,n}\\ \dot{x}'_{R,n}=c\dot{x}_{R,n}\\ x'_{R,n}=c^2x_{R,n}\\ t'_n=ct_n\Rightarrow\tau'=c\tau\end{cases} \tag{A3}$$

fulfills the requirements of TOE for Eq. (1). For any constant, c, the primed variables also fulfill Eq. (1), which can be verified by inserting them into these equations. This implies that by choosing $c=1/t_n$ each periodic racket ball-bouncing system is normalized by h to unit period without changing its dynamical properties. Hence, due to h, any further analysis of ball bouncing can be performed on one system with unit period. For the present analyses it is important that the scaling relation does not affect the acceleration of the racket. Thus, acceleration at impact can directly serve as a measure of local stability.

Nonlocal stability

To obtain more differentiated predictions for the $\ddot{x}_{R,n}$ values across the large range of $\ddot{x}_{R,n}$, the most common method is a nonlocal stability analysis of an equilibrium point. In this analysis a Lyapunov function is found which is a potential function of the state variables and which is formulated to have a global minimum at this equilibrium point. If the time derivative of this potential function is always negative, i.e., its value monotonically decreases with time, the system converges to the minimum of the Lyapunov function. Since, by definition, the minimum is the equilibrium point, global stability of the system is proven. For a nonlinear system a Lyapunov function candidate can be derived from the linearized system (e.g., [13]). The candidate function, L_n, for the linearized dynamical system is:

$$L_n=\mathbf{x}_{B,n}^{\mathbf{T}}\mathbf{P}\mathbf{x}_{B,n}. \tag{A4}$$

To obtain negative time derivatives, the matrix **P** has to satisfy the equation

$$\mathbf{A}^{\mathbf{T}}\mathbf{P}\mathbf{A}-\mathbf{P}=-\mathbf{I}. \tag{A5}$$

A is the system matrix of Eq. (A1) and **I** is the identity matrix. For the discretized system, the value of L_n must continuously decrease when $x_{B,n}$ is recursively iterated through Eq. (1). Thus, a ΔL can be defined between two successive impacts n and $n+1$ of ball and racket: $\Delta L=L_{n+1}-L_n=\mathbf{x}_{B,n+1}^T\mathbf{P}\mathbf{x}_{B,n+1}-\mathbf{x}_{B,n}^T\mathbf{P}\mathbf{x}_{B,n}$, where the nonlinear system Eq. (1) must be inserted for $\mathbf{x}_{B,n+1}$. For any state $\mathbf{x}_{B,n}$, ΔL may serve as a measure of how quickly the ball will converge to the stable equilibrium point. While negative values of ΔL indicate that $\mathbf{x}_{B,n}$ lies in the basin of attraction, a single positive ΔL characterizes $\mathbf{x}_{B,n}$ as unstable.

Using numerical optimization analysis it is possible to assess these stability properties by simulating the dynamics of the racket bouncing system given by Eq. (1). At time $t=0$ an equilibrium point was defined to be at the impact position, $x_R=0$, and the bouncing period was set to $\tau=0.4$ s. The scaling relation h ensures that these values can be chosen arbitrarily without losing generality of the results. The locally relevant section of the racket trajectory around the equilibrium point was modeled as a sixth-order polynomial in time (the order 6 was empirically determined to give sufficient accuracy for the given purpose): $x_R(t)=c_0+c_1t+c_2t^2+c_3t^3+c_4t^4+c_5t^5+c_6t^6$.

For the given impact conditions, $x_R(t=0)=0$, c_0 must be zero. The constant c_1 is also determined, because the racket velocity at impact is fully determined by the ballistic flight and the coefficient of restitution. At impact the second derivative of the polynomial equation is $\ddot{x}_R(t=0)=2c_2$. This acceleration was set to 20 different values, taken from the range of local stability. The goal of the optimization was to adjust the constants c_3 to c_6 for each of the 20 $\ddot{x}_R(t=0)$ to achieve the largest and steepest basin of attraction for the equilibrium point. Values of ΔL were calculated by starting the ball at 2500 different initial conditions in the vicinity of the equilibrium point. The sum of all 2500 ΔL's for a given

set of parameters, $\Sigma\Delta L$, was defined as an operational measure quantifying stability for each $\ddot{x}_R(t=0)$. The ball's initial conditions were determined by different deviations from the impact time, $t=0$, and impact velocities around the equilibrium point of $\ddot{x}_R$. The range of the initial values was chosen to cover an appropriately large neighborhood around the equilibrium point, but, as this calculation aimed to give relative evaluations of $\ddot{x}_R$, the actual range limits could be chosen freely: $t_{\text{init}} \in [-0.18\tau, +0.18\tau]$, $\dot{x}_{B,\text{init}} \in [-4\ \text{ms}^{-1}, -1\ \text{ms}^{-1}]$. The initial conditions were obtained by discretizing the intervals into 50 values each. The optimization was performed with Powell's conjugate gradient method [14].

Figure 3 shows the numerical results of $\Sigma\Delta L$ as a function of $\ddot{x}_R(t)$. Note that small $\Sigma\Delta L$ correspond to high global stability. As the trajectory of the racket corresponding to each of the different $\ddot{x}_R(t)$ was optimized to obtain maximal stability, the results express the best possible case for each $\ddot{x}_R(t)$. Stability is closely related to variability, since weakly stable states are accompanied with larger fluctuations than highly stable states and have longer relaxation times when perturbed. Therefore, the variability of $\ddot{x}_{R,n}$ should increase proportional to the numerical estimate of the global stability index, $\Sigma\Delta L$.

[1] N. B. Tufillaro, T. Abbott, and J. Reilly, *An Experimental Approach to Nonlinear Dynamics and Chaos* (Addison-Wesley, Redwood City, CA, 1992), and references therein; J. Guckenheimer and P. Holmes, *Nonlinear Oscillations, Dynamic Systems, and Bifurcations of Vector Fields* (Springer, New York, 1983).

[2] E. Fermi, Phys. Rev. **75**, 1169 (1949).

[3] M.-O. Hongler, P. Cartier, and P. Flury, Phys. Lett. A **135**, 106 (1989).

[4] S. Celaschi and R. L. Zimmermann, Phys. Lett. A **120**, 447 (1987); C. R. de Oliveira and P. S. Goncalves, Phys. Rev. E **56**, 4868 (1997).

[5] S. Schaal and C. G. Atkeson, *IEEE International Conference on Robotics and Automation, Atlanta 1993* (IEEE, Piscataway, NJ, 1993), Vol. 3, p. 913.

[6] S. Schaal, D. Sternad, and C. G. Atkeson, J. Motor Behavior **28**, 165 (1996).

[7] P. J. Beek and M. T. Turvey, J. Exp. Psychol. Hum. Percept Perform **18**, 934 (1992).

[8] A. J. Lichtenberg and M. A. Lieberman, Physica D **1**, 291 (1980).

[9] P. Pieransky and R. Bartolino, J. Phys. (France) **46**, 687 (1985).

[10] In this experiment we calculated median and quartile range instead of mean and standard deviations, as the small data sets sometimes did not satisfy the assumption of a normal distribution. The median is defined as that score point at or below which 50% of the data fall. The quartile range is the dispersion estimate, which is defined as the range of the variable where 25% of the data above and 25% data below the median fall.

[11] E. A. Jackson, *Perspectives in Nonlinear Dynamics* (Cambridge University Press, New York, 1989), Vol. 1.

[12] V. I. Arnol'd, *Geometrical Methods in the Theory of Ordinary Differential Equations* (Springer, Berlin, 1983).

[13] T. -C. Chen, *Linear Systems Theory and Design* (Holt, Rinehart and Winston, Orlando, FL, 1984).

[14] W. H. Press, B. P. Flannery, S. A. Teukolsky, and W. T. Vetterling, *Numerical Recipes in C - The Art of Scientific Computing* (Cambridge University Press, Cambridge, MA, 1988).